Tensile behavior of new 2,200 MPa and 2,400 MPa strands according to various types of mono anchorage

Jin Kook Kim[1a], Taek Ryong Seong[1b], Kyung Pil Jang[2c] and Seung Hee Kwon[*2]

[1]*Energy Infrastructure Research Department, Steel Structure Research Division, Research Institute of Industrial Science and Technology, POSCO Global R&D Center, Incheon, Republic of Korea*
[2]*Department of Civil and Environmental Engineering, Myongji University, Yongin, Republic of Korea*

Abstract.   High-strength strands are widely used as a key structural element in cable-stayed bridges and prestressed concrete structures. Conventional strands for stay cable and tendons in prestressed concrete structures are ϕ15.7mm coated seven-wire strands and ϕ15.2mm uncoated seven-wire strands, respectively, but the ultimate strengths of both strands are 1860MPa. The objective of this paper is to investigate the tensile behavior of a newly developed ϕ15.7mm 2,200 MPa coated strand and a ϕ15.2mm 2,400 MPa uncoated strand according to various types of mono anchorages and to propose appropriate anchorages for both strands. Finite element analyses were initially performed to find how the geometry of the anchor head affects the interaction among the anchor head, the wedge and the strand and to find how it affects the stress distributions in both parts. Tensile tests for the new strands were carried out with seven different types of mono anchorages. The test results were compared to each other and to the results obtained from the tensile tests with a grip condition. From the analysis and the test results, desirable mono anchorages for the new strands are suggested.

Keywords: high-strength strand; 2,200 MPa; 2,400 MPa; tensile test; mono anchorage; pre-stressed concrete; cable-stayed bridge

1. Introduction

   High-strength seven-wire strands have been in common use as key structural elements, specifically as a component of tendons and cables, in prestressed concrete members and cable-stayed or suspension bridges, respectively. In prestressed concrete members such as concrete girders, slabs, LNG storage tanks, containment structures of nuclear power plants, floating structures, and cross-beams of pylons in suspension and cable-stayed bridges, compressive pre-stressing is generally introduced over the potential tensile region by applying tensile force to tendons to prevent the concrete from cracking and to enhance structural performances. In cable-stayed bridges, the cables are connected to girders, and loads including the self-weight of the

---
*Corresponding author, Associate Professor, E-mail: kwon08@mju.ac.kr
[a]Senior Researcher, E-mail: jinkook.kim@rist.re.kr
[b]Senior Principal Researcher, E-mail: trseong@rist.re.kr
[c]Research Assistant, E-mail: k6851p@naver.com

girders and other live loads are fully or partially transferred to the pylons through the cables.

Existing types of strands that are commonly adopted in practice have a nominal strength of 1,860 MPa. Recently, two types of seven-wire strands were developed with nominal strengths of 2,400 MPa and 2,200 MPa. The strand with a strength of 2,400 MPa was designed for use in the post-tensioning of concrete members or structures; its diameter and nominal cross-sectional area are 15.2 mm, and 138.7 mm^2, respectively. The other strand with a strength of 2,200 MPa was targeted for use as a cable in cable-stayed bridges; its diameter and nominal cross-sectional area are 15.7mm and 150.0 mm^2, respectively. Each wire of the strands for stay cables is coated with zinc and aluminum, and the strands have a waxed extruded plastic coating to protect them from corrosion. Both strands also contain a wire rod composed of 0.98% carbon and 1.3% silicon. The wire rod undergoes drawing and twisting to become the 2,400 MPa strand. The stay cable strand undergoes a process identical to that of the 2,400 MPa strand while also undergoing an additional coating process, after which the strength is reduced to 2,200 MPa owing to the heat generated during the coating process

The structural performance measures, i.e., the safety, serviceability, and durability, greatly depend on the mechanical properties of the structural constituents. A high-strength construction material enables a reduction in the size of the structural members and the total amount of required materials, but it may also decrease the safety redundancy of the structures when they become more slender with the use of such a material. Therefore, when a new construction material is introduced in the construction field, the mechanical properties of the new material should be experimentally verified (Paik and *et al.* 2011, Wang and Liu 2012, Kwon and Shah 2008, Kwon *et al.* 2007).

In the process of developing new strands, the tensile mechanical performance is examined through tensile tests in which the end parts of the specimens are fixed with a special grip. However, the actual end condition imposed on strands may be quite different from those by the grips used in a laboratory test because an anchorage consisting of a steel block with a hole, known as an anchor head, as well as wedges are commonly used continually to sustain the tensile force applied to the strands for the life of the structures. The tensile behavior of strands is greatly influenced by the end condition due to the stress concentration resulting from the wedge and slippage between the block and the wedge. Therefore, it is necessary to determine the realistic tensile behavior of new strands under circumstances in which an anchorage system is imposed onto the end parts. In addition, a new anchorage may need to be devised for the new strands, as higher tensile force is introduced to these strands and because the anchorage should have a larger load-bearing capacity.

In the previous studies, three issues were concerned. The first is the material property of a newly developed Grade 300 (2160MPa) D12.7mm strand in comparison with 1860MPa D12.7mm and 15.2mm strands. Even though the strength increased, the characteristics of the stress-strain relationship of the higher strength strands was found to be identical to the others (Hill 2006, Loflin 2008). The second is the method of testing prestressed concrete wire strand. It is difficult to avoid stress concentration near strand grip during the tensile test which can affect strength and stress-strain relationship of a strand. Some researches investigated effect of variables such as eccentricity between strand ends, loading rate, and initial stress, etc (Godfrey 1956, Preston 1985, Walsh 2009, Walsh *et al.* 2012). The third is the interaction between rod and wedge. In this case, CFRP with circular section was main interest (Terrasi *et al.* 2011, Al-Mayah *et al.* 2013). However, the behavior of anchorage for steel strand is highly affected by the interaction between wedge and anchor head along with the stress concentration in strand near the tip of wedge because the strand is tightly grasped by the teeth on the inner surface of wedge and monolithic behavior of the strand

and wedge is made.

The objective of this study is to investigate the tensile behavior of new strands according to various types of mono anchorage blocks. Finite element analyses are initially performed to determine how the shape of the anchor block affects the behavior of the strands. Then, tensile tests of new strands are carried out with seven different mono anchorage types. The test results are compared to each other and to the results obtained from conventional tensile tests with a grip condition. From the analysis and the test results, desirable mono anchorages for new strands are proposed.

2. Numerical review of the shape of the mono anchor head

2.1 General

Strands have much higher ultimate strengths, ranging from 1,720 MPa to 2,400 MPa, compared to a conventional structural steel of which the highest ultimate strength ranges from 800 MPa to 1,000 MPa. The mono anchorage consists of an anchor head with a length of 50 mm and a wedge, of which the ultimate strengths are less than 600 MPa (Sétra 2006, Sétra 2009). The inside face of the wedge has saw teeth that can grasp the strands efficiently. The wedge slides into the hole of the anchor head as the tensile force is introduced to the strand, and the wedge, the strand and the anchor head behave as one structural body after a certain amount of the tensile force is applied to the strand. In the process of introducing tensile force to the strand, it is inevitable that the stresses acting on the wedge and the anchor head become locally concentrated and exceed the yield stress. The level of stress concentration and the position at which the yield occurs depend on the shape of the anchor head. A nonlinear finite element analysis was performed to investigate how the shape of the anchor head influences the tensile behavior. The test variables were also determined based on the analysis results.

Three different shapes of the anchor head are considered in the analysis. Fig. 1 shows the cross-section of the anchor head, and Table 1 gives the dimensions of the anchor heads considered in the analysis here, denoted as AH1, AH2, and AH3. AH1 is the conventional size of the anchor head; the outer diameter D is increased in AH2, while the height H is increased in AH3.
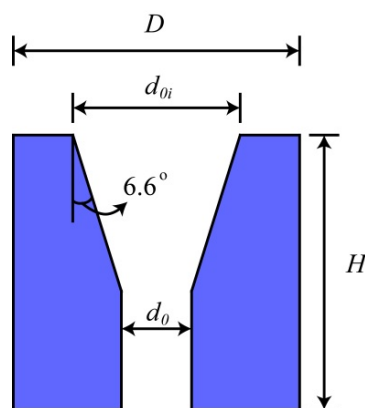

Fig. 1 Dimension of the anchor head

Table 1 Types of anchor heads

Type		D (mm)	H (mm)	d_i (mm)	d_o (mm)
F.E.M.	AH1	50	50	29	18
+	AH2	55	50	29	18
Tests	AH3	50	55	29	18
	AH4	50	50	29	19.5
Tests	AH5	50	50	29.5	18.5
	AH6	50	50	29.5	19.5
	AH7	48.9	50	29	19.5
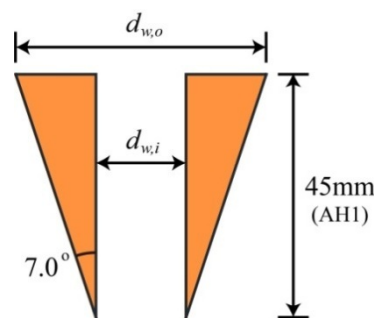
Fig. 2 Dimensions of the wedge

Table 2 Type of wedges

Type	$d_{w,o}$ (mm)	$d_{w,i}$ (mm)
w1	29	15.2
w2	29	15.7

Fig. 2 shows the cross-section of the wedge. Its dimensions are listed in Table 2. The numerical analysis focused on the effect of variations of the anchor head geometry. For this reason, only the strand with the strength of 2,400 MPa was considered in the analysis. A wedge, denoted as w1, is included in the analysis. The angle of the wedge is 0.3° greater than the angle of the inclined face on the anchor head. The modeling and the analysis were performed with a commercial program, ABAQUS Ver. 6.10.

2.2 Modeling

The strand, wedge, anchor head were modeled as separate bodies, as show in Fig. 3, and an eight-node solid element was used for the individual body. The saw teeth were ignored, and the contacting faces between the wedge and the strand were tied. A penalty algorithm and the interference fit were employed to consider the contact behavior between the wedge and the anchor head (Noh *et al*. 2012). Tensile force of 333 kN corresponding to the nominal strength of 2400 MPa pertaining to the strand was applied to the end of the strand while the anchor head was fixed on a rigid plate. Before applying the tensile force, the initial position of the wedge was assumed to protrude 2.0 mm from the top of the anchor head. The friction coefficients between the outer face of the wedge and the inner face of the anchor head and between the anchor head and the rigid plate were assumed to be 0.3 (Noh *et al*. 2012).
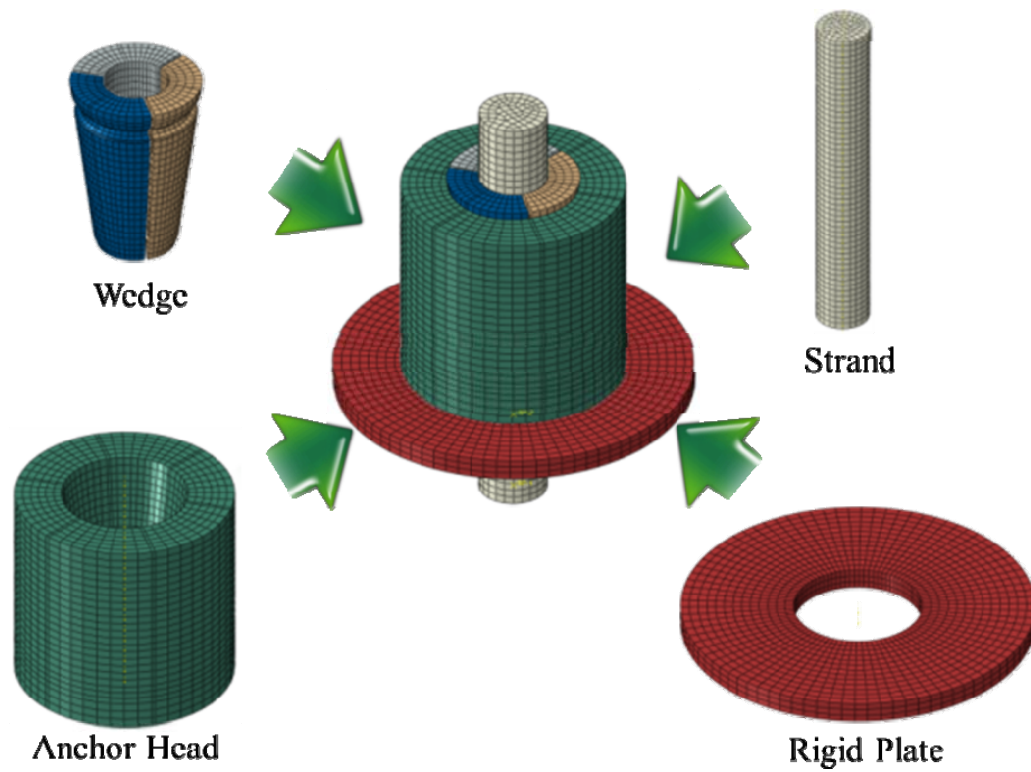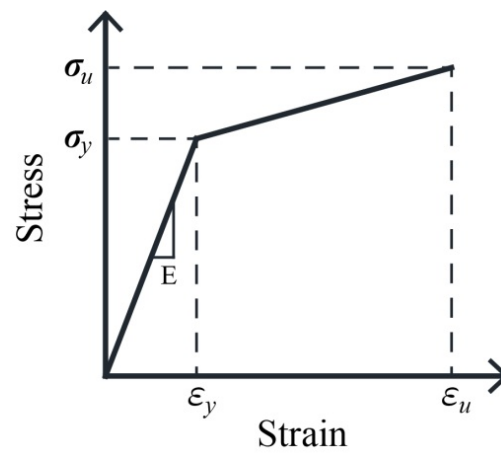
Fig. 3 Finite element model

Fig. 4 Stress-strain relationship used in the analysis

Table 3 Material properties used in the analysis

Part	σ_y (MPa)	σ_u (MPa)	ε_u (%)	E (GPa)
Strand	2,040	2,400	3.5	
Wedge	500	600	12	200
Anchor Head	343	520	20	

The anchor head and the wedge are made of the carbon steel for structural use and chrome molybdenum steel, respectively (KS D 3752 2007, KS D 3867 2007, Noh *et al*. 2012). The manufacturer does not usually provide the mechanical properties of the two materials because both materials experience processes such as heat treatment and drawing. In addition, it is difficult experimentally to measure the typical mechanical properties of these materials because the structural shapes of the anchor head and the wedge are very complex. The mechanical properties of the strand, the wedge, and the anchor head are assumed to be a bilinear curve, as illustrated in Fig. 4 and described in Table 3.

2.3 Analysis results

Fig. 5 shows the Von Mises stress distributions at the maximum load stage. The maximum Von Mises stress occurs at the surface of the strand located at the end of the wedge. These values are 2,087 MPa, 2064 MPa, and 2,097 MPa respectively for AH1, AH2, and AH3. For AH2, the outer diameter of the anchor head is 55 mm, 5 mm larger than that of AH1. The increased diameter provides greater confinement to the upper part of the wedge, which plays serves to reduce the concentration of the stress in the lower part of the wedge. On the other hand, for AH3, the

(a) AH1 (2,087MPa)   (b) AH2 (2,064MPa)
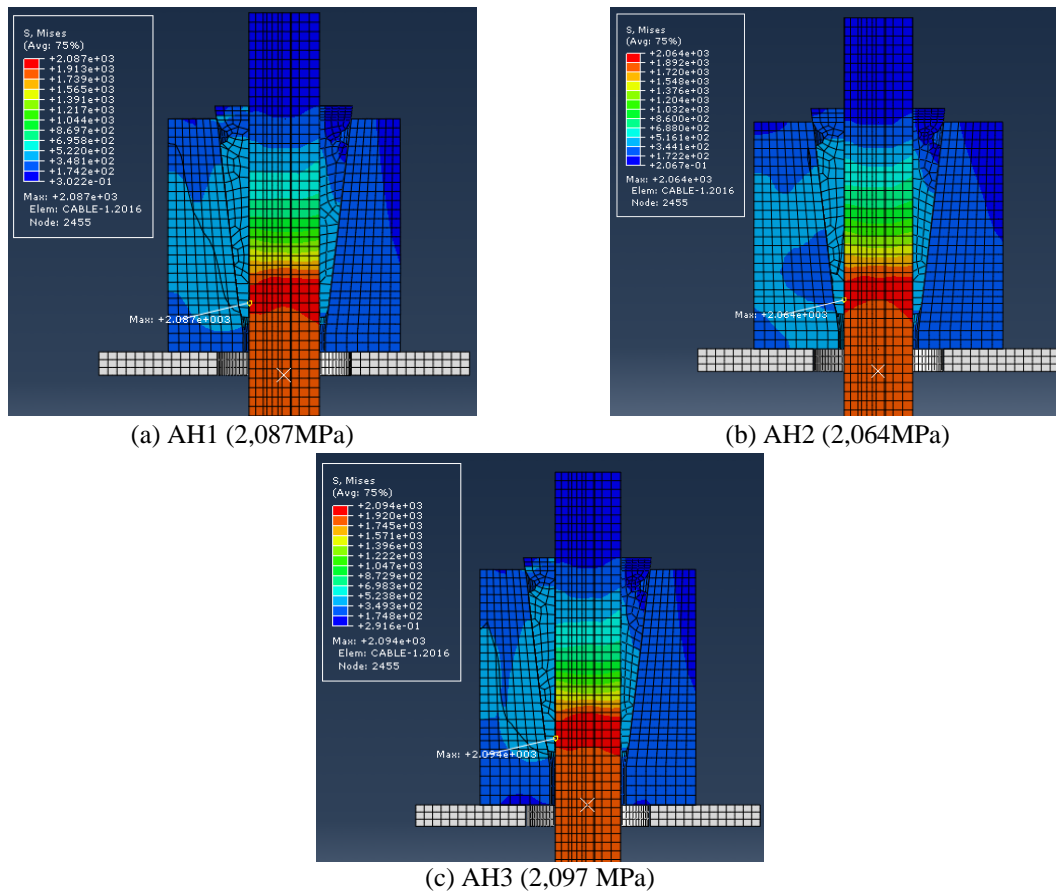
(c) AH3 (2,097 MPa)

Fig. 5 Von Mises stress distribution according to the shape of the anchor head

increased height of the anchor head increases the stiffness of the lower part of the anchor head, and the stress becomes more concentrated in the lower part due to the increased stiffness. The analysis showed that the increased outer diameter of the anchor head is more efficient in reducing the stress concentration, which may cause failure of the strand in the mono anchorage.

3. Experiments

3.1 Test program

Although numerical analyses of anchorages were attempted in earlier work (Seo *et al*. 2010a, b, Terrasi and *et al*. 2011, Noh *et al*. 2012, Al-Mayah 2013), accurately estimating the actual behavior of the anchorages is limited due to a combination of sophisticated nonlinearities, such as the surface contact between the strand and the wedge, the friction between the wedge and the anchor head, the localized yielding, and the confinement due to the anchor head. For this reason, the mechanical performance of the new anchorage should be experimentally examined according to a specified method (PTI 1998, EOTA 2002).

The tensile tests for the strands with the ultimate strength levels of 2,400 MPa and 2,200 MPa were performed with a grip and different types of anchor heads and wedges, as listed in Table 4. Regarding the strand with the strength of 2,400 MPa, a total of five cases of one grip condition and four different anchor heads were tested with three companion specimens. In the tests of the strand with the strength of 2,200 MPa, a total of eight cases of one grip condition, six anchor heads and two wedges were considered with three companion specimens except in the S2-AH5-W2 case. The types of anchor heads and wedges are shown in Tables 1 and 2. In the tests of both strands, the three anchor heads AH1, AH2, and AH3 considered in the numerical analysis were included. AH7 was included in the test of strand S1 to examine the effect of the outer diameter and the internal diameter (d_0) on the stress concentration. The anchor heads AH4, AH5, and AH6 were the test variables used to assess the effect of the internal diameters (d_0, d_{0i}).

Table 4 Test program

Designation of Specimen	Strand		End Condition	Wedge	The Number of Companion Specimens
	Strength, f_{pu} (MPa)	Diameter, d_s (mm)			
S1-G			G[*]	-	3
S1-AH1-w1			AH1	w1	3
S1-AH2-w1	2,400 (S1)	15.2	AH2	w1	3
S1-AH3-w1			AH3	w1	3
S1-AH7-w1			AH7	w1	3
S2-G			G	-	3
S2-AH1-w1			AH1	w1	3
S2-AH1-w2			AH1	w2	3
S2-AH2-w2	2,200 (S2)	15.7	AH2	w2	3
S2-AH3-w2			AH3	w2	3
S2-AH4-w2			AH4	w2	3
S2-AH5-w2			AH5	w2	2
S2-AH6-w2			AH6	w2	3

G[*]: Epoxy-filled aluminum tube grip

3.2 Test methods

There were two types of tensile tests; the first used a grip to hold the strand at the end of the specimen and the second was the test of the mono anchorage. In the former test, the end parts of the strands were protected by the epoxy-filled aluminum tube, which is considered to be an efficient method to prevent the formation of a notch (Godfrey 1956, Hill 2006, Podolney 1967, Preston 1985, Preston 1990). The length of the grip holding the test specimen was 100mm. Fig. 6 shows the test setup for the test with a grip. Fig. 7 is the test setup for the tests with the mono anchorages. The anchor heads were fixed with a special jig, as shown in Fig. 7(b).

A universal testing machine with a capacity of 1,000 kN was used, as shown in Fig. 6(c) and Fig. 7(c), and the elongation of the strand was measured at the cross-head of the actuator. Every test proceeded up to the failure of the strand, as shown in Fig. 8.

The fracture of the strand wires usually happens inside the anchorage, more specifically, within the first few full-depth wedge teeth where the strand entered into the anchor because of the stress concentration (Walsh and Kurama 2012). On the other hand, in the perfect grip condition, the fracture occurs in the free length of the seven wires (Walsh 2009).

(a) Epoxy-filled aluminum tube

(b) Grip

(c) test setup

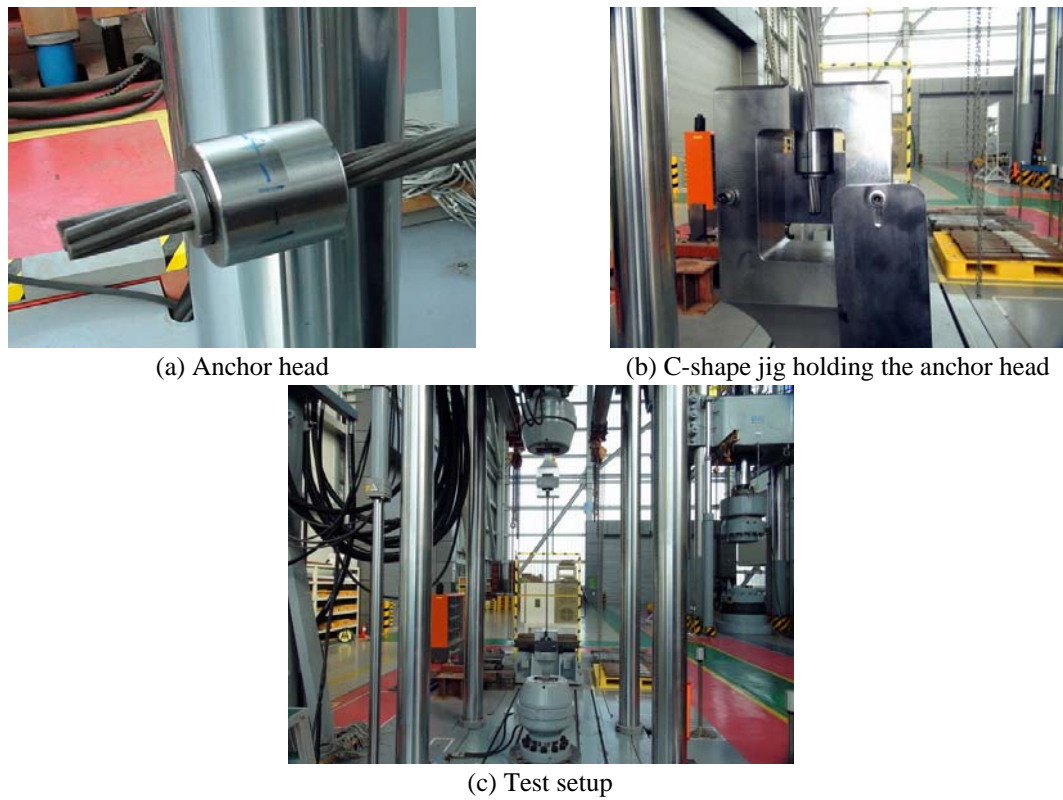Fig. 6 Test setup for tensile tests with a grip

(a) Anchor head

(b) C-shape jig holding the anchor head

(c) Test setup

Fig. 7 Test setup for the tensile tests with mono anchorage

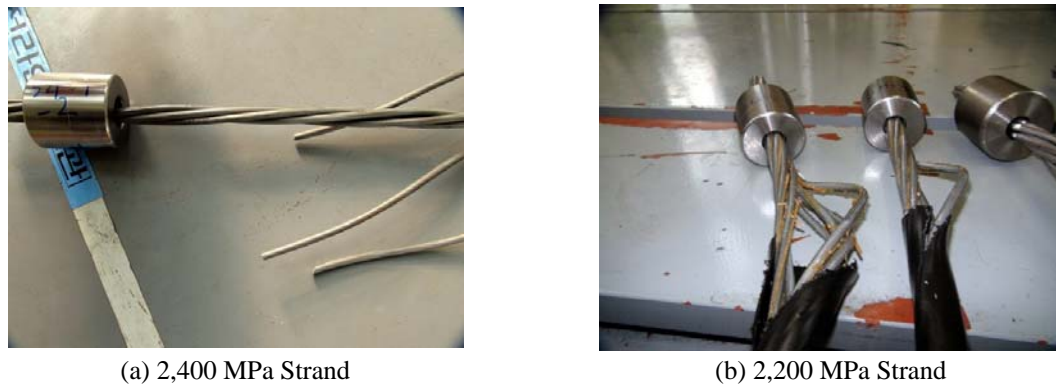(a) 2,400 MPa Strand

(b) 2,200 MPa Strand

Fig. 8 Failure of the strands

4. Results and discussion

4.1 Tensile behavior of new strands in the grip condition

Fig. 9 shows the measured relationship between the load and the strain in the tensile test with the grip condition. The horizontal line indicates the load corresponding to the nominal strength.

The yield stresses at 0.1 % and 0.2 % offsets, the ultimate strength, and the elongation at the ultimate strength are listed in Table 5. In every test result, the ultimate strength exceeded the nominal strength. The minimum elongation for the 2,400 MPa tendon was 7.18 %, which satisfies the specification that the elongation shall be greater than 3.5 % (ASTM A 416). The load-strain relationship of 2,400 MPa strand shows similar behavior to those of lower grade strands (Hill 2006, Loflin 2008).

The specification for stay cables states that the elongation should be larger than 4.5 %. However, only one of the three 2,200 MPa strand specimens fulfilled that specification. The small amount of elongation may have resulted from the fact that during the test, an extensometer was not installed; therefore, the strain calculated from the displacement of the cross head may be underestimated. In addition, a rupture of the strand occurred in the vicinity of the grip. The results for the 2,200 MPa strand in the grip condition will not be used to represent the mechanical performance of the strand; these results are only used for a comparison with the test results of the mono anchorages.
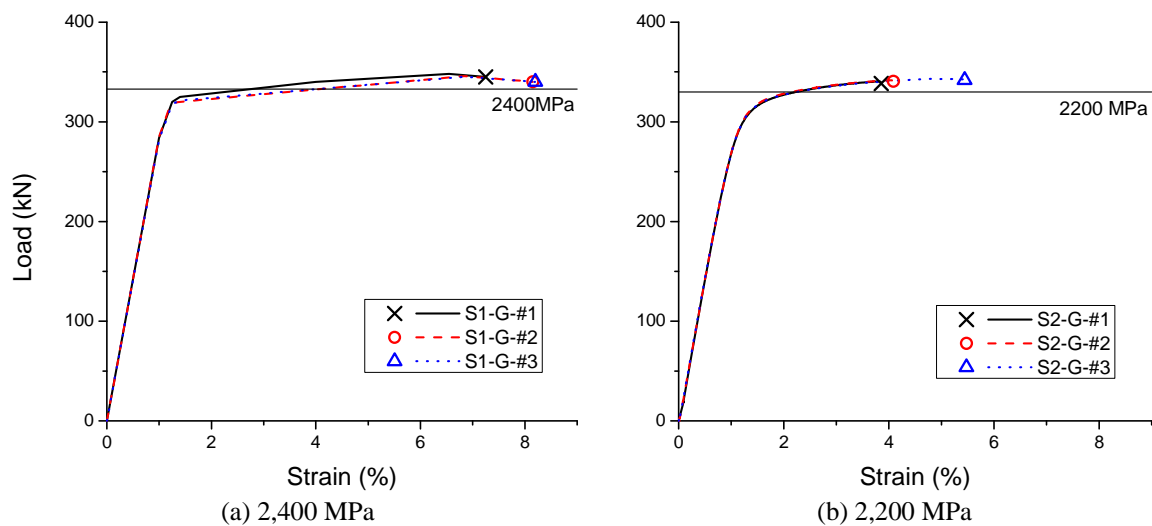

Fig. 9 Tensile test results in the grip condition

Table 5 Mechanical properties of new strands obtained from tensile tests with the grip

Specimen		Yield Stress at 0.1% offset (MPa)		Yield Stress at 0.2% offset (MPa)		Ultimate Strength (MPa)		Elongation (%)		Elastic Modulus (GPa)	
S1-G	#1	2,305	2,288 (Avg.)	2,344	2,324 (Avg.)	2,503	2,495 (Avg.)	7.18	7.86 (Avg.)	200.7	198.3 (Avg.)
	#2	2,270		2,312		2,492		8.24		201.1	
	#3	2,290		2,317		2,490		8.15		193.2	
S2-G	#1	2,199	2,199 (Avg.)	2,251	2,251 (Avg.)	2,270	2,279 (Avg.)	3.85	4.46 (Avg.)	194.6	193.1 (Avg.)
	#2	2,199		2,252		2,278		4.09		192.2	
	#3	2,199		2,251		2,288		5.44		192.5	

4.2 Tensile behavior of 2,400 MPa strand in the mono anchorages

The test results for the 2,400 MPa strands in the mono anchorages are depicted in Fig. 10, and the maximum loads and the elongations are summarized in Table 6. In all of the specimens, the measured ultimate strength and the elongation amounts exceed the nominal strength of 2,400 MPa and the nominal elongation of 3.5%, respectively. When the strands failed, it was observed that the rupture of one or more wires occurred at the tip of teeth of the wedge.

The averaged maximum load and the averaged elongation for the AH2 case were largest, and the values for AH3 were lowest among AH1, AH2, and AH3. As mentioned in the numerical analysis, this result was attributed to the fact that the increased outer diameter in AH2 provides greater confinement over the upper part of the wedge. Moreover, the increased height in AH3 leads to greater confinement over the lower part of the wedge.

In the AH7 case, the maximum load and the elongation were even lower than in the AH3 case. The confinement over the upper part of the wedge was reduced due to the smaller outer diameter of AH7. The increased inner diameter in the lower part of the anchor head shortens the
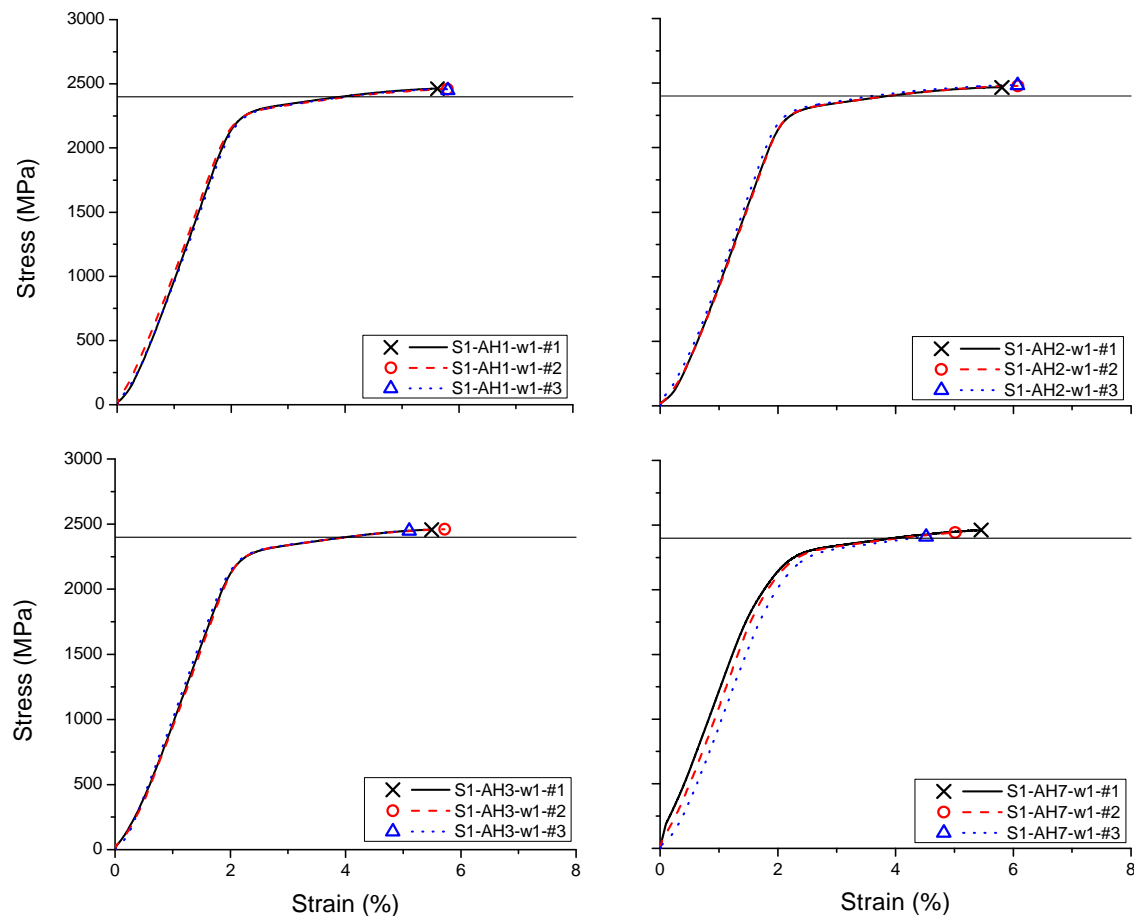

Fig. 10 Tensile test results for the 2,400 MPa strand in the mono anchorage

Table 6 Measured maximum loads and elongations for the strands of 2,400 MPa

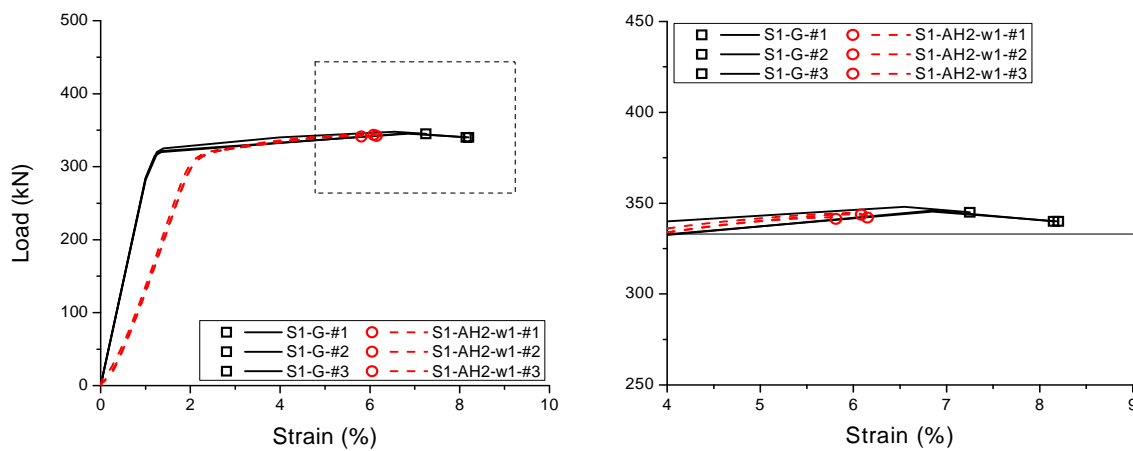| Designation of Specimen	Maximum Load (kN)				Elongation (%)			
	#1	#2	#3	Average (MPa)	#1	#2	#3	Average
S1-G	347.2	345.6	345.3	346.0 (2,495)	7.18	8.24	8.15	7.86
S1-AH1-w1	341.5	341.0	341.3	341.3 (2,461)	5.61	5.74	5.67	5.67
S1-AH2-w1	342.3	343.8	344.6	343.6 (2,477)	5.73	5.91	5.97	5.87
S1-AH3-w1	340.9	341.3	339.6	340.6 (2,456)	5.45	5.68	5.09	5.41
S1-AH7-w1	341.4	338.8	334.3	338.2 (2,438)	5.45	5.00	4.52	4.99

Fig. 11 Comparison between the test results of S1-G and S1-AH1-w1

length of the inclined line in the upper part of the anchor head; that is, the area of the contact surface between the wedge and the anchor head is reduced. The reduced contact area may lead to greater stress concentration at the lower part of the wedge. In addition, the relatively large deviation of the results in AH7 may be attributed to the fact that the smaller contact areas of AH7 between the anchor head and the test jig, and between the anchor head and wedge might be more sensitive to a stress concentration.

According to the specification of the anchorage (PTI 1998, EOTA 2002), the maximum stress applied to the strand with the anchorage should exceed 95 % of the guaranteed ultimate tensile strength or 95 % of the actual ultimate tensile strength, and the elongation should be larger than a strain of 2% based on the displacement of the cross head. As a result, the conventional mono anchorage, AH1, can be used for the new strand with the strength of 2,400 MPa. It was also experimentally confirmed that the increase in the outer diameter in the anchor head is efficient in reducing the stress concentration between the wedge and the strand.

A comparison between the test results of S1-G1 and S1-AH2-w1 is shown in Fig. 11, in which the dotted box in the graph on the left is magnified on the right. The initial slope of S1-G is much steeper than that of S1-AH2-w1. The lower slope in the mono anchorage is caused by slippage between the wedge and the anchor head. However, after the yield point, the slopes for the grip and the anchorage are nearly identical, indicating that slippage does not occur after yielding. The earlier rupture in the anchorage may be caused by the stress concentration between the wedge and the strand.
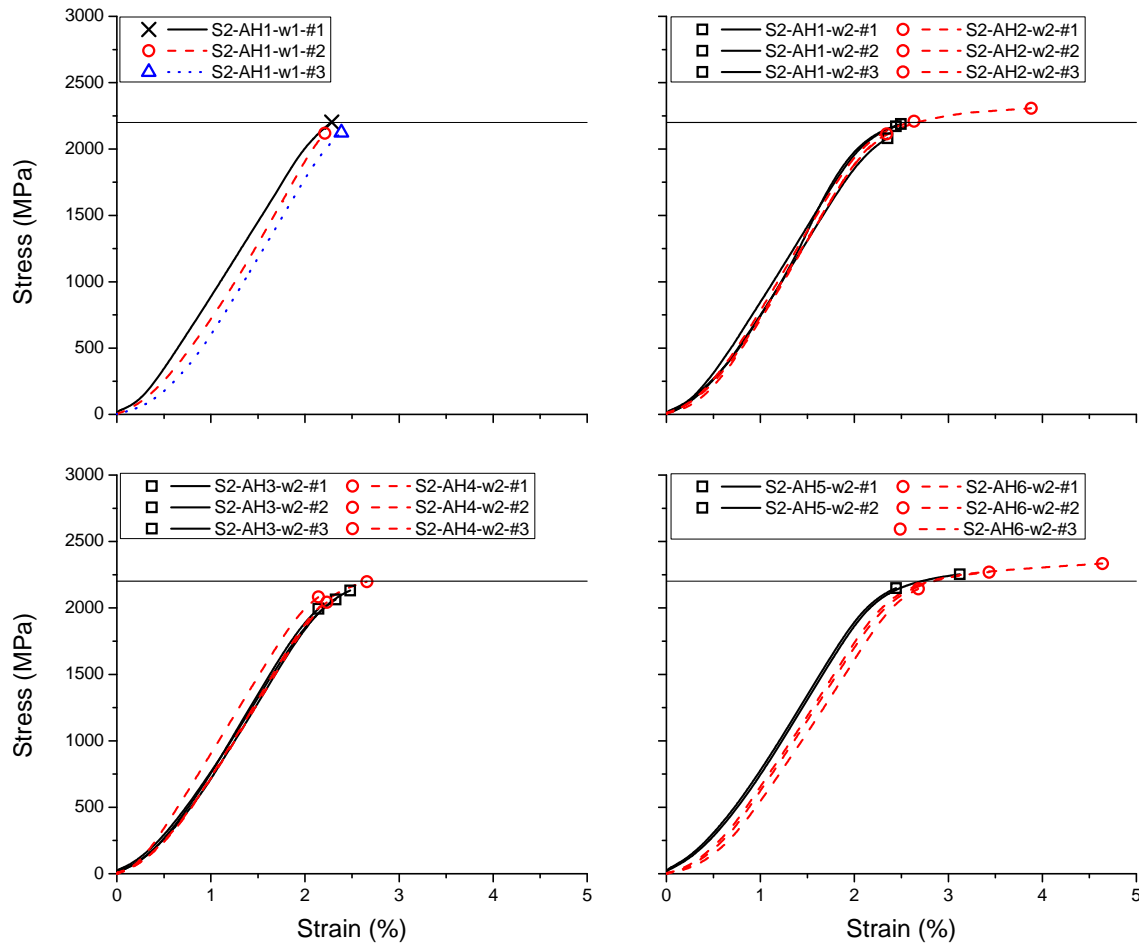
Fig. 12 Tensile test results for the 2,200 MPa strand in the mono anchorage

4.3 Tensile behavior of the 2,200 MPa strand in the mono anchorages

The measured stress-strain relationships of 2,200MPa strands in the mono anchorages are shown in Fig. 12. The horizontal lines in the graphs denote the nominal strength of 2,200 MPa. In contrast to the result from the 2,400 MPa strand, some specimens exceed the nominal strength while others do not. This indicates that the mono anchorages used in the tests cannot be employed for the 2,200 MPa strands. When the strands failed, similarly to the strands of 2,400 MPa, it was observed that the rupture of one or more wires occurred at the tip of teeth of the wedge.

The strand consists of seven wires. One wire is located in the center, and the other six circumferential wires are twisted around the center wire. When the strand is subjected to tension force during the tensile test, the force or the stress should be uniformly distributed over all of the wires to attain full performance of the strand. If a uniform distribution is not attained, the wire on which the stress is more concentrated may fail or fracture first. In this case, the accurate strength of the strand cannot be measured in the test. In the test, while the force exerted by the wedge is

Table 7 Measured maximum loads and elongations for the strands of 2,200 MPa

Designation of Specimen	Maximum Load (kN)				Elongation (%)			
	#1	#2	#3	Average (MPa)	#1	#2	#3	Average
S2-G	340.5	341.7	343.2	341.8 (2,279)	3.95	4.25	5.60	4.60
S2-AH1-w1	305.5	293.8	294.7	294.2 (2,121)	2.28	2.21	2.39	2.30
S2-AH1-w2	325.7	328.2	312.2	322.0 (2,147)	2.44	2.49	2.35	2.43
S2-AH2-w2	331.5	317.1	346.0	331.5 (2,210)	2.64	2.34	3.88	2.95
S2-AH3-w2	309.6	319.6	299.0	309.4 (2,063)	2.33	2.48	2.14	2.32
S2-AH4-w2	312.2	306.5	329.6	316.1 (2,107)	2.14	2.23	2.66	2.34
S2-AH5-w2	322.4	337.9	-	330.2 (2,201)	2.44	3.12	-	2.78
S2-AH6-w2	350.1	321.6	340.4	331.0 (2,207)	4.64	2.68	3.43	3.06

directly transmitted to the outer six wires, the center wire is pulled by friction force at the interface between the center wire and the other six wires. The friction force is generated by confinement force, specifically the normal force acting on the side surface of the center wire. If the friction coefficient between the wires is not large enough, relative displacement between the center wire and the other six wires is induced as the force exerted in the strand increases, resulting in a lower failure load than the nominal strength. A lubricating agent can prevent corrosion but may hinder the friction between the wires. Furthermore, the lubricating agent is supposed to cause more variability in the behavior of the strand because the deviation of test results for 2,200 MPa strand is much larger than the 2400MPa strand.

The maximum loads and the elongations are listed in Table 7. The maximum load and the elongation for the S2-AH1-w1 case were lowest, indicating that the wedge for the strand with the diameter of 15.2 mm is not appropriate for a larger strand. Like the results for S1-AH1-w1, S1-AH2-w1, and S1-AH3-w1, the maximum stress and the elongation are greater in the order of S2-AH2-w2, S2-AH1-w2, and S2-AH3-w2. The effects of the increased outer diameter and the increased height of the anchor head on the behavior of the 2,200 MPa strand are comparable to those in the case of the 2,400 MPa strand.

The internal diameter in the lower part of the anchor head is larger in AH4 compared to AH1. As mentioned above, the increased inner diameter reduces the contact area between the wedge and the anchor head. The reduced contact area induces a greater stress concentration at the lower part of the wedge. In reality, the maximum load and the elongation for S2-AH4-w2 were lower than those for S2-AH1-w2, as shown in Table 7. In contrast, the increased inner diameter at the top of the anchor head enlarges the contact area. The enlarged contact area can lead to a more uniform stress distribution between the strand and the wedge. In the test results, the maximum loads and the elongations for S2-AH5-w2 and S2-AH6-w2 are larger than those for S2-AH4-w2, as shown in Table 7.

A comparison between the test results of S2-G2 and S2-AH2-w2 was done, as shown in Fig. 13, similarly to Fig. 11. It was also observed that the slippage between the wedge and the anchor head occurs from the beginning of loading and stops near the yielding point. Meanwhile, a greater stiffness discrepancy between the grip condition and the anchorage condition at the ends of the strands is observed in Fig. 13. This can be explained by the fact that the wax in the strand and the slippage in the anchorage reduced the friction between the center wire and the six circumferential wires and the additional deformation induced in the six wires. On the other hand, in the grip condition, the epoxy was filled into the aluminum tube in a hot liquid state and permeated the
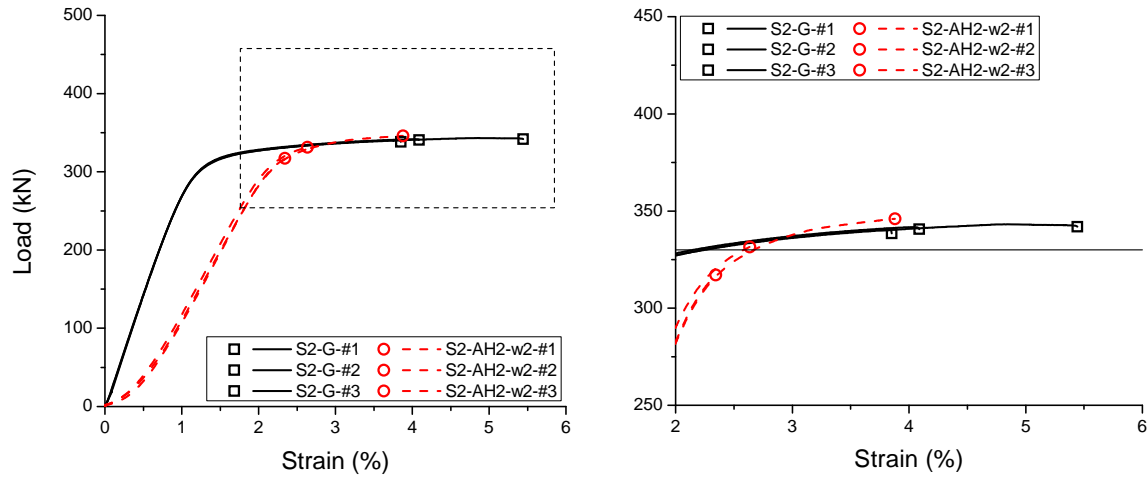
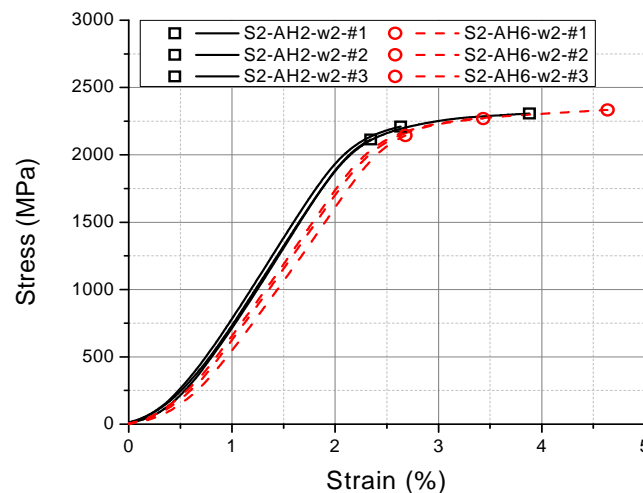Fig. 13 Comparison between the test results of S2-G and S2-AH2-w2

Fig. 14 Comparison between the test results of S2-AH2-w2 and S2-AH6-w3

space between the wires by melting and extruding the wax. This is a common process to ensure the monolithic behavior of the wires.

In the tensile tests with the anchorage, the stress limit is 95 % of the guaranteed ultimate tensile strength, which corresponds to 313.5 kN, while the elongation limit is 2 %. The test cases in which the criteria for the maximum stress and the elongation were satisfied in all three companion specimens were S2-AH2-w2 and S2-AH6-w2, of which the test results are compared in Fig. 14. The slope from the initial loading point to the yield point is larger in the anchorage of S2-AH2-w2. The steeper slope indicates that the slippage between the wedge and the anchor head is minor. In practice, less slippage is more efficient when seeking to reduce the initial loss of the tensile force applied to the strand. Thus, the mono anchorage of S2-AH2-w2 is preferred for the 2,200 MPa strand among the anchorages tested in this study.

5. Conclusions

In this study, the tensile behavior of new strands with the strengths of 2,400 MPa and 2,200 MPa according to various types of mono anchorages were investigated. From a numerical analysis and from experiments, the following conclusions can be drawn.

• The conventional mono anchorage can be used for the strand with the strength of 2,400 MPa but not for the strand with the strength of 2,200 MPa.

• An anchor head with an outer diameter of 5 mm larger than a conventional anchor head is suggested for strands with strength levels of 2,200 MPa.

• The increased outer diameter of the anchor head provides more confinement to the upper part of the wedge, which plays a role in reducing the concentration of the stress in the lower part of the wedge.

• The increased height of the anchor head increases the stiffness of the lower part of the anchor head, and the stress becomes more concentrated in the lower part due to the increased stiffness.

• The wedge for a strand with a diameter of 15.2 mm is not suitable for a strand with a diameter of 15. 7 mm.

• The increased inner diameter of the lower hole in the anchor head reduces the contact area between the wedge and the anchor head. The reduced contact area induces a greater stress concentration at the lower part of the wedge.

• The increased inner diameter at the top of the anchor head plays a role in enlarging the contact area. An enlarged contact area can lead to a more uniform stress distribution between the strand and the wedge.

• The wax in the strand for stay cables may reduce the friction between the center wire and the six circumferential wires and induce additional deformation in the six wires.

Acknowledgements

References

Al-Mayah, A., Soudki, K. and Plumtree, A. (2013), "Towards a simplified anchor system for CFRP rods", *Journal of Composites for Construction*. (in press)
ASTM International (2012), "Standard Specification for Steel Strand, Uncoated Seven-Wire for Prestressed Concrete", ASTM A416, USA
EOTA (2002), "Guideline for European Technical Approval of Post-Tensioning Kits for Prestressing of Structures (ETAG 013)", EOTA, Brussels.
Fib (2005), "Acceptance of stay cable systems using prestressing steels", *International Federation for Structural Concrete fib*, Lausanne, Switzerland.
Godfrey, H.J. (1956), "The physical properties and methods of testing prestressed concrete wire strand", *PCI Journal*, **1**(3), 38-47.

Hill, A.T. Jr. (2006), "Material properties of grade 300 and grade 270 prestressing strands and their impact on the design of bridges", M.S. Thesis, Virginia Polytechnic Institute and State University, Blacksburg, VA.

ISO 15630-3 (2010), "Steel for the reinforcement and prestressing of concrete - Test methods - Part 3: prestressing steel", *The International Organization for Standardization*, Switzerland.

Kim, J.K., Lee, P.G. and Lee, M.S. (2010), "Development of 2,160MPa strand and application technology", *Magazine of Korea Concrete Institute*, **25**(1), 68-70. (in Korean)

KS D 7002 (2011), "Uncoated stress-relieved steel wires and strands for prestressed concrete", Korean Standards Association, Seoul, Korea.

KS D 3752 (2007), "Carbon steel for machine structural use", Korean Standards Association, Seoul, Korea.

KS D 3867 (2007), "Low-alloy steels for machine structural use", Korean Standards Association, Seoul, Korea.

Kwon, S.H. and Shah, S.P. (2008), "Prediction of early-age cracking of fiber-reinforced concrete due to restrained shrinkage", *ACI Materials Journal*, **105**(4), 381-389.

Kwon, S.H., Ferron, R.P., Akkaya, Y. and Shah, S.P. (2007), "Cracking of fiber-reinforced self-compacting concrete due to restrained shrinkage", *International Journal of Concrete Structures and Materials*, **1**(1), 3-9.

Loflin, B.J. (2008), "Bond and material properties of grade 270 and grade 300 prestressing strands", Master Degree Thesis at Virginia Polytechnic Institute and State University, Virginia, USA.

Noh, M.H., Seong, T.R. and Kim, J.K. (2012), "Nonlinear analysis of anchor head for high strength steel strand", *COSEIK Journal*, **25**(2), 163-174.

Paik, I.Y., Shim C.S., Chung, Y.S. and Sang, H.J. (2011), "Statistical properties of material strength of concrete, re-bar and strand used in domestic construction site", *Journal of the Korea Concrete Institute*, **23**(4), 421-430. (in Korean)

Preston, H.K. (1985), "Testing 7-wire strand for prestressed concrete-the state of the art", *PCI Journal,* **30**(3), 134-155.

Preston, H.K. (1990), "Handling prestressed concrete strand", *PCI Journal*, **35**(6), 68-71.

PTI (1998), "Acceptance Standards for Post-Tensioning Systems", Post-Tensioning Institute, Phoenix, USA.

PTI (2012), "Recommendations for Stay Cable Design, Testing, and Installation", Post-Tensioning Institute, Phoenix, USA.

Seo, J.W., Jeong, W. and You, H. (2010), "Socket design and safety review on PPWS cable for suspension bridge", *2010 KSCE Conference Proceedings*, 2517-2517. (in Korean)

Seo, J.W., Jeong, W., Cho, E.K. and You**, H.** (2010), "Parametric analysis to determine optimum geometries of PPWS sockets in cable-suspension bridges", *2010 KSCE Conference Proceedings*, 35-36. (in Korean)

Sétra (2009), "European Technical Approval No ETA-09/0068", Sétra, Bagneux Cedex, France.

Sétra (2006), "European Technical Approval No ETA-06/0006", Sétra, Bagneux Cedex, France.

Terrasi, G.P., Affolter, C. and Barbezat, M. (2011), "Numerical optimization of a compact and reusable pretensioning anchorage system for CFRP tendons", *Journal of composites for construction,* **15**(2), 126 - 135.

Walsh, K.Q. and Kurama, Y.C. (2012), "Effects of loading conditions on the behavior of unbonded post-tensioning strand-anchorage systems", *PCI Journal*, 76-86.

Walsh, K.Q. (2009), "Behavior and design of unbonded post-tensioning strand/anchorage systems for seismic applications", Master Degree Thesis at University of Notre Dame, Indiana, USA.

Wang, X.H. and Liu, X.L. (2012), "Analysis of RC beam with unbonded or exposed tensile reinforcements and defective stirrup anchorages for shear strength", *Computers and Concrete*, **10**(1), 59-78.